Research Square

Preprints are preliminary reports that have not undergone peer review.
They should not be considered conclusive, used to inform clinical practice,
or referenced by the media as validated information.

Crystal Structures of Phenyl-Extended Pillar[5]arene: Guest Inclusion, Cavity Flexibility, and Supramolecular Assembly

Randa Abd Almoaeen
Kuwait University
Mickey Vinodh
Kuwait University
Fatemeh H. Alipour
Kuwait University
Talal F. Al-Azemi
t.alazemi@ku.edu.kw

Kuwait University

Research Article

Keywords: Phenyl-extended pillar[5]arene, inclusion complexes, supramolecular assembly, Hirshfeld surface analysis

Posted Date: November 19th, 2026

DOI: https://doi.org/10.21203/rs.3.rs-11493283/v1

License: This work is licensed under a Creative Commons Attribution 4.0 International License.
Read Full License

Additional Declarations: No competing interests reported.

Crystal Structures of Phenyl-Extended Pillar[5]arene: Guest Inclusion, Cavity Flexibility, and Supramolecular Assembly

Randa Abd Almoaeen, Mickey Vinodh, Fatemeh H. Alipour, and Talal F. Al-Azemi*

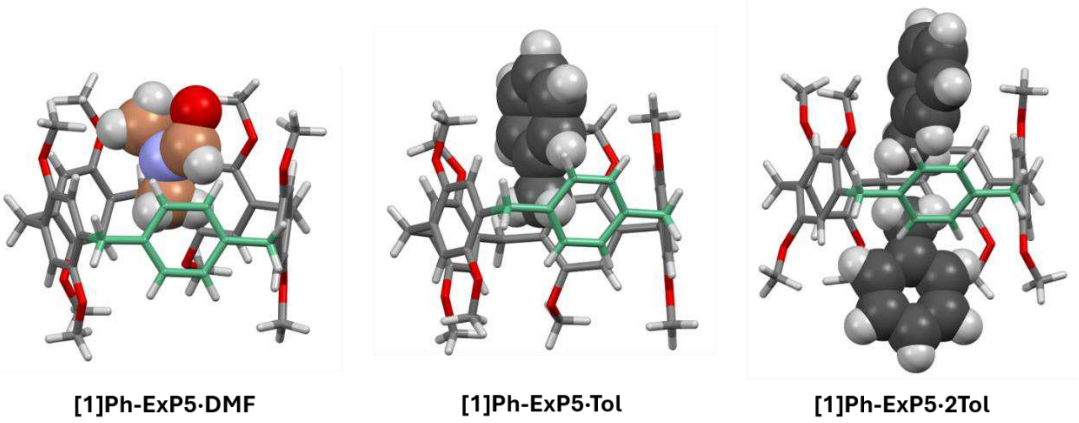
Chemistry Department, Kuwait University, P.O. Box 5969, Safat 13060, Kuwait

e-mail: t.alazemi@ku.edu.kw

Abstract

The crystal structures of phenyl-extended pillar[5]arene ([**1]Ph-ExP5**) obtained under different crystallization conditions were determined by single-crystal X-ray diffraction to examine its conformational flexibility, guest inclusion, and supramolecular organization. Two guest-free crystalline forms exhibit subtle differences in macrocyclic conformation and distinct intermolecular association patterns, forming supramolecular dimers and one-dimensional supramolecular polymers, respectively. The two toluene inclusion complexes, **[1]Ph-ExP5·Tol** and **[1]Ph-ExP5·2Tol**, accommodate one and two toluene molecules within the macrocyclic cavity, respectively. Structural comparison indicates that outward rotation of the unsubstituted phenyl unit expands the cavity, allowing the inclusion of two toluene molecules. In the **[1]Ph-ExP5·DMF** complex, interactions involving DMF molecules link dimeric host–guest assemblies into one-dimensional chains. The resulting supramolecular assemblies were fully characterized using single-crystal X-ray diffraction and Hirshfeld surface analysis.

Graphical abstract



Keywords: Phenyl-extended pillar[5]arene; inclusion complexes; supramolecular assembly; Hirshfeld surface analysis.

Introduction

Pillar[n]arenes and their functional derivatives have emerged as versatile macrocyclic hosts in supramolecular chemistry owing to their well-defined cavities, readily tunable functional groups, and host–guest recognition capabilities [1–5]. Structural modified pillar[n]arenes has attracted considerable interest as a strategy for tailoring cavity geometry, modulating host–guest interactions, and expanding the functional diversity of these macrocyclic systems [6–17]. Among these derivatives, phenyl-extended pillar[n]arenes, in which one or more 1,4 dimethoxybenzene units of the conventional permethylated pillar[n]arene framework are replaced by unsubstituted phenyl units, constitute an intriguing class of structurally modified macrocycles [18–21].

The incorporation of unsubstituted phenyl units is expected to influence the molecular geometry and conformational preferences of the parent macrocycles. In particular, the absence of methoxy substituents may reduce local steric congestion and provide additional conformational freedom, potentially modifying the shape, dimensions, and accessibility of the macrocyclic cavity. Furthermore, the altered steric and electronic environments may influence intermolecular association and host–guest recognition through non-covalent interactions, including π–π stacking, C–H···π, and C–H···O interactions. These structural features make phenyl-extended pillar[n]arenes attractive systems for investigating the relationship between macrocyclic conformation, guest inclusion, and supramolecular assembly.

From a crystallographic perspective, the structural asymmetry introduced by phenyl extension provides an opportunity to examine how variations in macrocyclic conformation and guest identity influence host–guest geometries and intermolecular interactions in the solid state. The nature and orientation of encapsulated guest molecules may be associated with conformational adjustments of the host, while the resulting intermolecular contacts can contribute to different supramolecular association motifs and crystal structures. Comparative single-crystal X-ray diffraction studies of different crystalline forms are therefore valuable for understanding the structural adaptability of these macrocycles and the factors governing their solid-state organization.

In the present study, we investigate the structural characteristics and supramolecular interactions of phenyl-extended pillar[5]arene (**[1]Ph-ExP5**) through single-crystal X-ray diffraction analysis of five crystalline forms obtained under different crystallization conditions, including guest-free forms and host–guest complexes containing toluene or N,N dimethylformamide (DMF). Comparative analysis of these structures focuses on macrocyclic conformation, cavity geometry, guest inclusion, and intermolecular non-covalent interactions. Hirshfeld surface analysis is

additionally employed to characterize the distributions and relative contributions of intermolecular contacts. Collectively, these investigations provide insight into the structural adaptability of **[1]Ph-ExP5** and elucidate how guest identity and crystallization conditions are associated with variations in its host–guest interactions and supramolecular organization.

Experimental

Instrumentation

The single crystal data collection was made on Rigaku Rapid II (Japan) diffractometer by Mo-Kα radiation at room temperature. Nuclear magnetic resonance (NMR) spectroscopy was done by Bruker Avance II 600 MHz (Germany). Electron impact ionization (EI) mass spectrometry was performed using Thermo Scientific DFS High Resolution GC/MS (Germany) mass spectrometer.

Synthesis

Synthesis of 1,4-bis(2,5.Dimethoxybenzyl)benzene

1,4-Dimethoxybenzene (5.52 g, 40 mmol) was dissolved in freshly distilled dichloromethane (80 mL) and treated with aluminum chloride (1170 mg, 8.8 mmol). A solution of α,α^{I} dichloro-p-xylene (704 mg, 4 mmol) in dichloromethane (20 mL) was then added dropwise to the reaction mixture. The resulting solution was stirred at room temperature for 2 h and subsequently quenched with water. The organic layer was separated, washed successively with water and brine, and dried over anhydrous sodium sulfate. The solvent was removed under reduced pressure, and the residue was purified by flash column chromatography on silica gel (petroleum ether/dichloromethane = 60:40 v/v) to afford the product as a white powder (1.12 g, 65%). ^{1}H NMR (600 MHz, $CDCl_3$), δ: 3.70 (s, 6H), 3.75 (s, 6H), 3.89 (s, 4H), 6.63 (m, 2H), 6.68 (m, 2H), 6.77 (m, 2H), 7.09 (s, 4H). ^{13}C NMR (150 MHz, $CDCl_3$), δ: 30.0, 35.7, 55.8, 56.3, 111.4, 111.6, 117.0, 129.1, 131.4, 138.4, 151.9, 153.7. HRMS 451.1885 (calc. for $C_{28}H_{28}O_4Na$); 451.1864 (found).

Synthesis of phenyl-extended pillar[5]arene.

Paraformaldehyde (180 mg, 6.0 mmol), 1,4-bis(2,5-dimethoxybenzyl)benzene (567 mg, 1.50 mmol), and 1,4-dimethoxybenzene (70 mg, 0.5 mmol) were dissolved in dichloromethane (100 mL) and stirred under a nitrogen atmosphere for 10 min. Boron trifluoride diethyl etherate (296 μL, 2.2 mmol) was then added, and the reaction mixture was stirred for an additional 25 min at room temperature. The reaction was quenched with aqueous sodium hydroxide solution, and the organic layer was separated, washed successively with water and brine, and dried over anhydrous

sodium sulfate. The solvent was removed under reduced pressure, and the residue was purified by flash column chromatography on silica gel using a dichloromethane/ petroleum ether mixture (60:40 v/v) to afford the desired [1]phenyl-extended pillar[5]arene **([1]Ph-ExP5**), which eluted out as the first fraction. Yield: 238 mg, 23% (based on 1,4-bis(2,5-dimethoxybenzyl)benzene precursor).^{1}H NMR (600 MHz, $CDCl_3$), δ: 3.59 (d, J = 4.0 Hz, 12H), 3.63 (s, 6H), 3.68 (s, 6H), 3.79 (m, 10H), 6.56 (s, 2H), 6.72 (m, 4H), 6.78 (s, 2H), 6.90 (s, 4H). ^{13}C NMR (150 MHz, $CDCl_3$), δ: 29.8, 30.2, 35.8, 56.1, 56.1, 56.2, 56.2, 113.8, 114.3, 114.4, 114.8, 128.4, 128.5, 128.6, 128.6, 129.1, 139.1, 151.0, 151.1, 151.2. HRMS 690.3187 (calculated for $C_{43}H_{46}O_8$); 690.3195 (found).

Preparation of single crystals for X-ray diffraction

Single crystals of **[1]Ph-ExP5** were obtained under five different crystallization conditions: Slow solvent evaporation of **[1]Ph-ExP5** (10 mg) dissolved in 1 mL dichloromethane gave **[1]Ph-ExP5-D** in 3 days. A dichloromethane solution of pillar[5]arene (10 mg **[1]Ph-ExP5** dissolved in 0.5 mL dichloromethane) and diffuse with 5 mL methanol gave **[1]Ph-ExP5-P** in one week. Crystals of **[1]Ph-ExP5** were grown with toluene under two different condition. In one trial **[1]Ph-ExP5** (10 mg) was dissolved in neat toluene (0.5 mL) and heated this sample at 100°C for 10 minutes to make sure all solid compound has been dissolved. The mixture was then kept for slow solvent evaporation and crystals were grown in 1 week (**[1]Ph-ExP5.Tol2**). In another attempt **[1]Ph-ExP5** (10 mg) dissolved in dichloromethane (1 mL) and 2 drops of toluene was added to this mixture and kept for slow solvent diffusion with methanol (5 mL). Pillar[5]arene crystals were grown in 10 days (**[1]Ph-ExP5.Tol1**). In the final attempt **[1]Ph-ExP5** (10 mg) was dissolved in dichloromethane : DMF (90 : 10 v/v 0.5 mL) and kept for slow solvent evaporation. Single crystals were grown in one week (**[1]Ph-ExP5.DMF**).

Crystal refinement

Single-crystal X-ray diffraction data were collected on Rigaku Rapid II (Japan) diffractometer by Mo-Kα radiation at room temperature. The crystal data collected were processed by 'Crystalclear' software package. The structures were then solved by direct methods using 'CrystalStructure' crystallographic software package and the refinement was performed using SHELXL-2019/3 [22]. All non-hydrogen atoms were refined anisotropically and hydrogen atoms were refined using the riding model.

In **[1]Ph-ExP5-D**, the unsubstituted phenyl ring and the oppositely oriented dimethoxy-substituted phenyl ring exhibit positional disorder, whereby a minor-occupancy component of each ring occupies the crystallographic position of the other ring, indicating a mutual interchange

of their positions. This disorder was modeled using PART commands, with the major and minor components refined to occupancies of 81.6% and 18.4%, respectively. The geometries of the disordered components were maintained using SADI, DFIX, DANG, and FLAT restraints, while SIMU and DELU restraints were applied to control their anisotropic displacement parameters. Only the major component of the disordered fragments were considered in the evaluation of non-bonded interactions and the generation of molecular graphics.

In the **[1]Ph-ExP5.DMF** crystal, positional disorder was observed for the unsubstituted phenyl ring. The major and minor disorder components were refined with occupancies of 73.1% and 26.9%, respectively. SAME restraints were employed to maintain chemically reasonable geometries, while SIMU and DELU restraints were applied to control the anisotropic displacement parameters of the disordered components. Additionally, a DFIX restraint was used to refine the carbonyl bond length of the DMF guest molecule.

In the **[1]Ph-ExP5.Tol1** crystal, the toluene molecule located outside the pillar[5]arene cavity exhibited disorder at a special position and was refined using the PART -1 command. SIMU and DELU restraints were applied to control its thermal displacement parameters, while DFIX, DANG, and FLAT restraints were used to maintain the chemically reasonable geometry of the disordered toluene molecule. Furthermore, a DFIX restraint was applied to ensure the appropriate geometry of the toluene molecule encapsulated within the pillar[5]arene cavity.

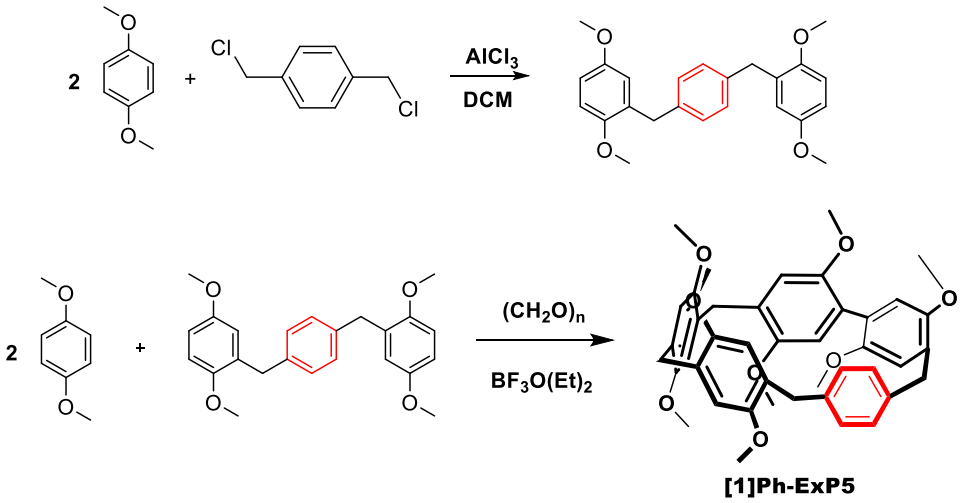
The asymmetric unit of the **[1]Ph-ExP5.Tol2** crystal contains two pillar[5]arene molecules and four toluene molecules. The geometries of the guest toluene molecules were refined using DFIX, DANG, and SADI restraints, while SIMU and DELU restraints were employed to control their anisotropic displacement parameters.

Molecular graphics and intermolecular interaction analyses were performed using Mercury (version 2024.3.0), while Hirshfeld surface analysis was conducted using CrystalExplorer 21.5 [23,24]. Only the major components of the disordered fragments were considered in the evaluation of non-bonded interactions and the generation of molecular graphics. Intermolecular contacts were assigned using conservative geometric criteria and are reported as potential interactions inferred from the molecular geometry rather than definitive evidence of specific intermolecular bonding. The cavity width was defined as the distance between the centroid of a phenyl ring and the opposite corner of the macrocyclic framework. The cavity height was determined by measuring the distance between the planes defined by the oxygen atoms at the upper and lower rims of the macrocycle. The crystallographic data for the structures reported in this paper has been deposited at the Cambridge Crystallographic Data Centre (2597661-2597665).

Results and Discussion

Crystal analysis of [1]phenyl-extended pillar[5]arene ([1]Ph-ExP5).

The synthesis of [1]phenyl-extended pillar[5]arene (**[1]Ph-ExP5**) is outlined in **Scheme 1**. Single crystals were obtained under five crystallization conditions: slow evaporation of dichloromethane (**[1]Ph-ExP5-D**) or neat toluene (**[1]Ph-ExP5.Tol1**), methanol vapor diffusion into a dichloromethane solution (**[1]Ph-ExP5-P**) or into a dichloromethane solution containing small amounts of toluene (**[1]Ph-ExP5.Tol2**) and slow evaporation of dichloromethane solution containing small amounts of DMF (**[1]Ph-ExP5.DMF**). Single-crystal X-ray diffraction analyses at room temperature revealed variations in the crystallographic parameters and supramolecular packing of the guest-free macrocycle and its toluene- and DMF-containing inclusion complexes, enabling investigation of the effects of guest inclusion and crystallization conditions on their solid-state organization.



Scheme 1: Synthesis of phenyl-extended pillar[5]arene (**[1]Ph-ExP5)**.

The crystal structures of **[1]Ph-ExP5-D** and **[1]Ph-ExP5-P**, obtained from dichloromethane by slow solvent evaporation and methanol diffusion, respectively, are devoid of solvent or guest molecules. Despite this similarity, the two crystal systems exhibit subtle differences in their structural features and supramolecular packing arrangements. In contrast, the crystal structures of **[1]Ph-ExP5.Tol1** and **[1]Ph-ExP5.Tol2** contain toluene molecules encapsulated within the macrocyclic cavities. Although both systems incorporate the same guest molecule, they differ in their crystallographic features and crystal packing arrangements. Similarly, the crystal structure of **[1]Ph-ExP5.DMF** reveals the inclusion of DMF molecules within the macrocyclic cavity. The crystal structures of all five systems are presented in **Fig. 1**, and their crystallographic data and

some of the macrocyclic features are summarized in **Table S1** to **Table S3** (supporting information).

Among these systems, crystal data similar to those **[1]Ph-ExP5-D** and **[1]Ph-ExP5.Tol2** have previously been reported in the literature [20], with their crystal structures determined at low temperature (CCDC deposition number 2103703 and 2103702). These systems are still included in the present study because the current crystallographic data were collected and analysed at room temperature. Their inclusion enables a comparative assessment of the crystallographic parameters and supramolecular features of all five crystal systems under the conditions considered in this work.

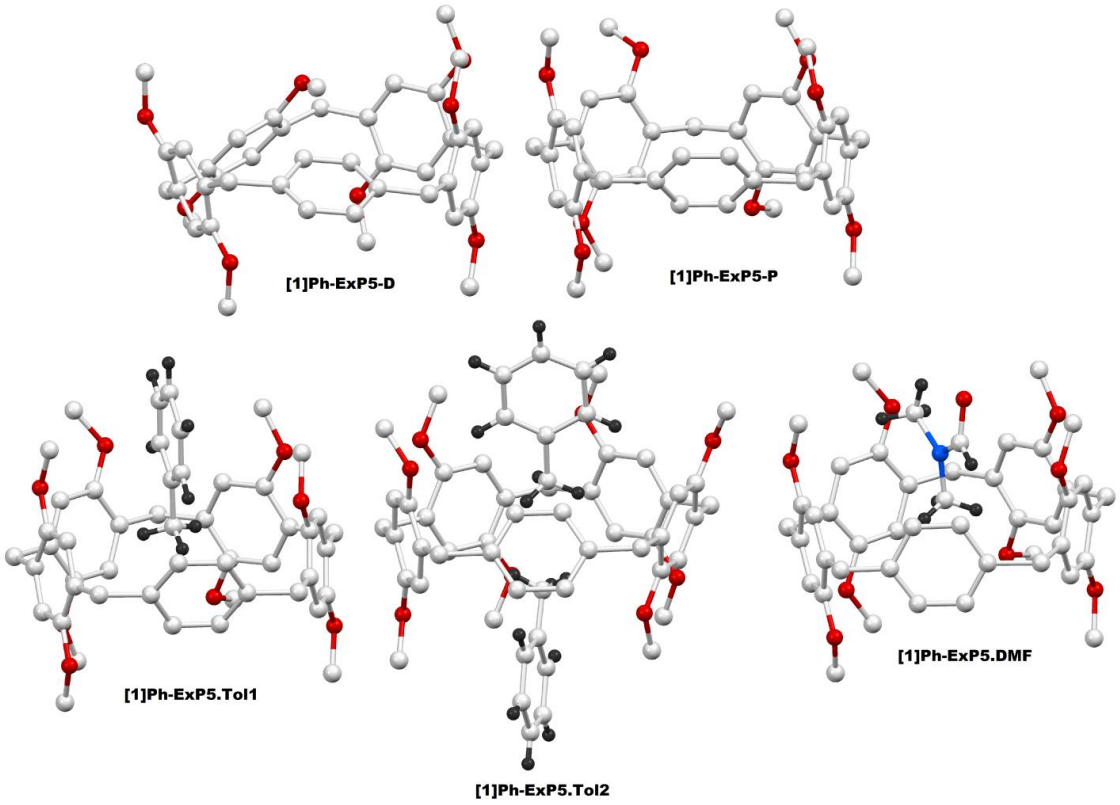


Fig. 1 Crystal structure of **[1]Ph-ExP5** systems obtained under different crystallization conditions. Hydrogen atoms except those belong to the guest molecules are omitted for clarity.

Crystal structures of [1]phenyl-extended pillar[5]arene with no guest species

The single-crystal structures of **[1]Ph-ExP5-D** and **[1]Ph-ExP5-P**, obtained by slow evaporation of dichloromethane and methanol diffusion, respectively, reveal solvent-free crystal structures in which no solvent or guest molecules are incorporated into the crystal lattice. Despite the absence of included solvent or guest species in both structures, subtle differences are observed in the conformational geometry of the pillar[5]arene macrocycles and their supramolecular packing

arrangements. In both crystals, the incorporation of an unsubstituted phenyl unit in place of one of the dimethoxy-substituted aromatic units of the conventional permethylated pillar[5]arene framework has a pronounced influence on the macrocyclic conformation. In conventional permethylated pillar[5]arenes, the five dimethoxy-substituted phenyl units typically adopt a near-perpendicular orientation relative to the mean plane of the macrocycle, with interplanar angles approaching 90°, thereby producing a relatively rigid, pillar-shaped architecture. This conformational arrangement can impose steric constraints on the accommodation of bulky aromatic guests. In contrast, the introduction of an unsubstituted phenyl unit modifies the steric environment and conformational preferences of the macrocyclic framework, resulting in distinct patterns of ring inclination and deviations from the idealized pentagonal geometry in **[1]Ph-ExP5-D** and **[1]Ph-ExP5-P**.

In the crystal structure of **[1]Ph-ExP5-D**, the unsubstituted phenyl ring exhibits a pronounced inward inclination towards the macrocyclic cavity, with a dihedral angle of 27.31° relative to the mean plane of the macrocycle (**Fig. 1** and **Fig. S6**, Supporting Information). The absence of methoxy substituents on this aromatic unit reduces local steric congestion and may facilitate greater conformational accommodation by the remaining dimethoxy-substituted phenyl rings. Among these rings, the dimethoxy-substituted phenyl unit located opposite the unsubstituted phenyl ring exhibits the greatest deviation from a perpendicular orientation, with an inclination angle of 43.14° relative to the mean macrocyclic plane. The remaining three dimethoxy-substituted phenyl rings retain comparatively near-perpendicular orientations, with corresponding dihedral angles of 77.76°, 83.95°, and 83.54°. The dihedral angles between the unsubstituted phenyl ring and its two adjacent dimethoxy-substituted phenyl rings are 78.53° and 80.67°, respectively. The pronounced inward inclination of the unsubstituted phenyl ring, together with the substantial deviation of the opposing dimethoxy-substituted phenyl ring from perpendicularity, results in a reduced cavity height of 4.105 Å. Furthermore, the distance from the centroid of the unsubstituted phenyl ring to the opposite corner of the macrocyclic framework is 8.57 Å, whereas the corresponding maximum distance from the centroid of a dimethoxy-substituted phenyl ring to the opposite corner is 9.44 Å. This disparity indicates a pronounced deviation from an idealized pentagonal arrangement and reflects the conformational distortion of the macrocycle in the solid state.

In the crystal structure of **[1]Ph-ExP5-P**, the unsubstituted phenyl ring is inclined towards the macrocyclic cavity at a dihedral angle of 46.15° relative to the mean macrocyclic plane (**Fig. 1** and **Fig. S7**, Supporting Information). This orientation differs substantially from that observed in **[1]Ph-ExP5-D**, where the corresponding angle is 27.31°. The four dimethoxy-substituted phenyl

rings in **[1]Ph-ExP5-P** exhibit inclination angles of 86.84°, 77.50°, 79.51°, and 89.24°, indicating that they retain relatively near-perpendicular orientations with respect to the mean macrocyclic plane. The dihedral angles between the unsubstituted phenyl ring and its two adjacent dimethoxy-substituted phenyl rings are 79.33° and 76.14°, respectively, values that are broadly comparable to those observed in **[1]Ph-ExP5-D**. The cavity height in **[1]Ph-ExP5-P** is 4.687 Å, which is greater than that in **[1]Ph-ExP5-D** (4.105 Å). This difference reflects the distinct conformational arrangements of the aromatic units in the two crystal structures, although the cavity height cannot be attributed solely to the inclination of the unsubstituted phenyl ring. The distance from the centroid of the unsubstituted phenyl ring to the opposite corner of the macrocycle is 8.96 Å, whereas the corresponding maximum distance from the centroid of a dimethoxy-substituted phenyl ring to the opposite corner is 9.12 Å. The smaller difference between these two distances, compared with that observed for **[1]Ph-ExP5-D** (8.57 and 9.44 Å, respectively), suggests a more uniform distribution of the macrocyclic dimensions and a closer approximation to the idealized pentagonal geometry in **[1]Ph-ExP5-P**.

Supramolecular interactions and crystal packing in [1]Ph-ExP5-D and [1]Ph-ExP5–P

In both **[1]Ph-ExP5-D** and **[1]Ph-ExP5-P**, the pillar[5]arene molecules engage in multiple intermolecular non-covalent interactions with symmetry-related neighboring macrocycles, resulting in distinct supramolecular assemblies. In the **[1]Ph-ExP5-D** crystal, two symmetry-related **[1]Ph-ExP5** molecules associate through eight C–H···π contacts and two C–H···O interactions to form a 1:1 supramolecular dimer (**Fig. 2**). In contrast, in the **[1]Ph-ExP5-P** crystal, each macrocycle interacts with two symmetry-related molecules positioned above and below the macrocyclic ring, generating a one-dimensional supramolecular chain (**Fig. 2**). This chain formation is mediated by two C–H···π contacts and one C–H···O contact at each intermolecular interface. Notably, the unsubstituted phenyl ring of the extended pillar[5]arene framework participates in C–H···π interactions in both crystal structures, contributing to the formation of the dimeric and one-dimensional supramolecular assemblies.

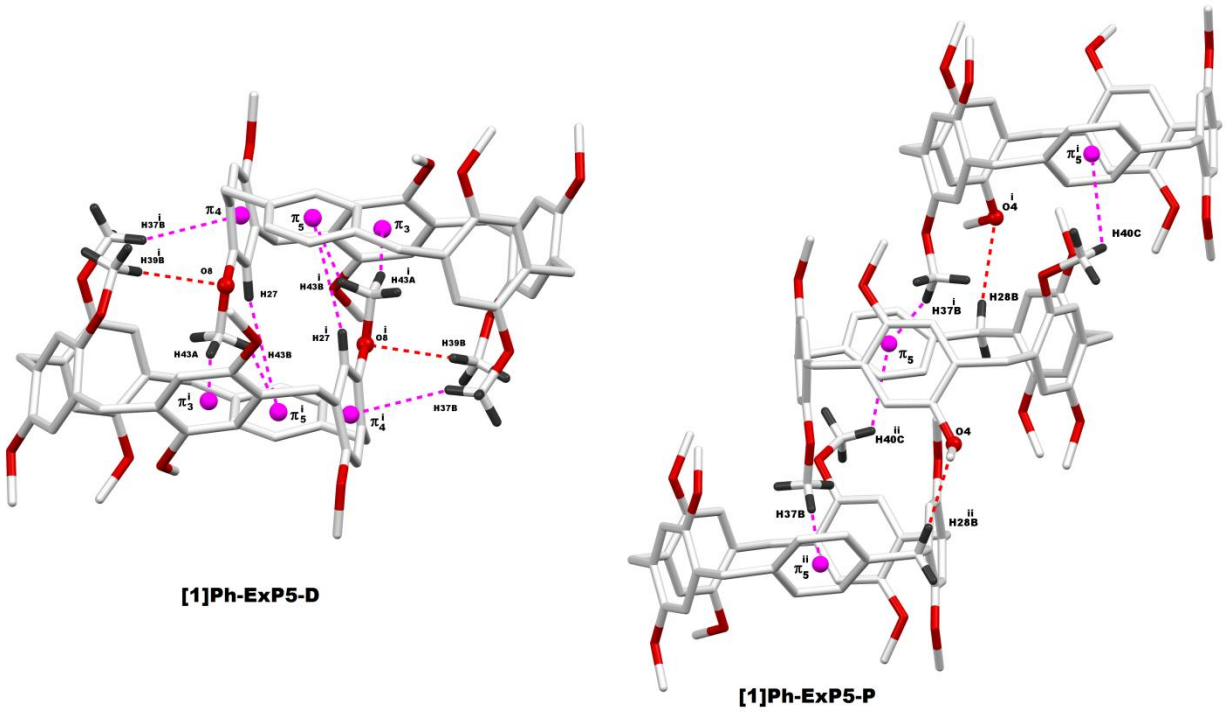


Fig. 2 Intermolecular non-bonding interactions (top-to bottom) observed among a pillar[5]arene molecule with its neighboring symmetry related counterparts resulted in supramolecular 1:1 dimer in **[1]Ph-ExP5-D** crystal and supramolecular linear polymer in **[1]Ph-ExP5-P** crystal. Symmetry code: (^{i}) 1-x, 1-y, 1-z; π3, π4 & π5 are the centroids of the phenyl rings C15-C20, C22-C27 & C29-C34 respectively (for **[1]Ph-ExP5-D**) and Symmetry code: (^{i}) x, 1/2-y, -1/2+z; (^{ii}) x, 1/2-y, 1/2+z; π5 is the centroids of the phenyl ring C29-C34 (for **[1]Ph-ExP5-D**).

Beyond these principal top-to-bottom associations, additional lateral intermolecular contacts contribute to the crystal packing in both structures. In **[1]Ph-ExP5-D**, each macrocycle engages in lateral C–H···O interactions with three symmetry-related macrocycles, as illustrated in **Fig. 3**. The lateral intermolecular connectivity is more extensive in **[1]Ph-ExP5-P**, where each macrocycle is in contact with eight neighboring symmetry-related macrocycles through C–H···π and C–H···O interactions (**Fig. 4**). Among these contacts, one C–H···π interaction and one C–H···O interaction exhibit complementary geometrical arrangements, as illustrated in **Fig. 4(B)**. The geometrical parameters of the top-to-bottom and lateral intermolecular contacts identified in the two crystal structures are summarized in **Tables 1** & **2**.

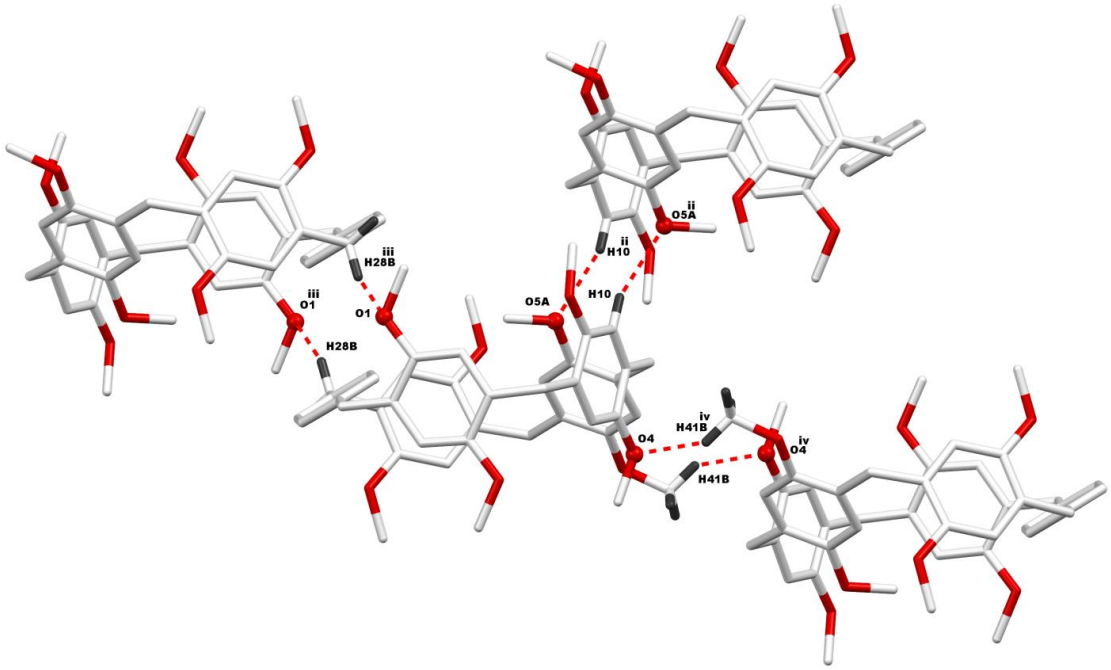


Fig. 3 Intermolecular non-bonding interactions (lateral) observed among a pillar[5]arene molecule with its neighboring symmetry related counterparts in **[1]Ph-ExP5-D** crystals. Symmetry code: ([ii]) -x, 1-y, 2-z; ([iii]) -x, 1-y, 1-z and ([iv]) 1-x, 1-y, 2-z.

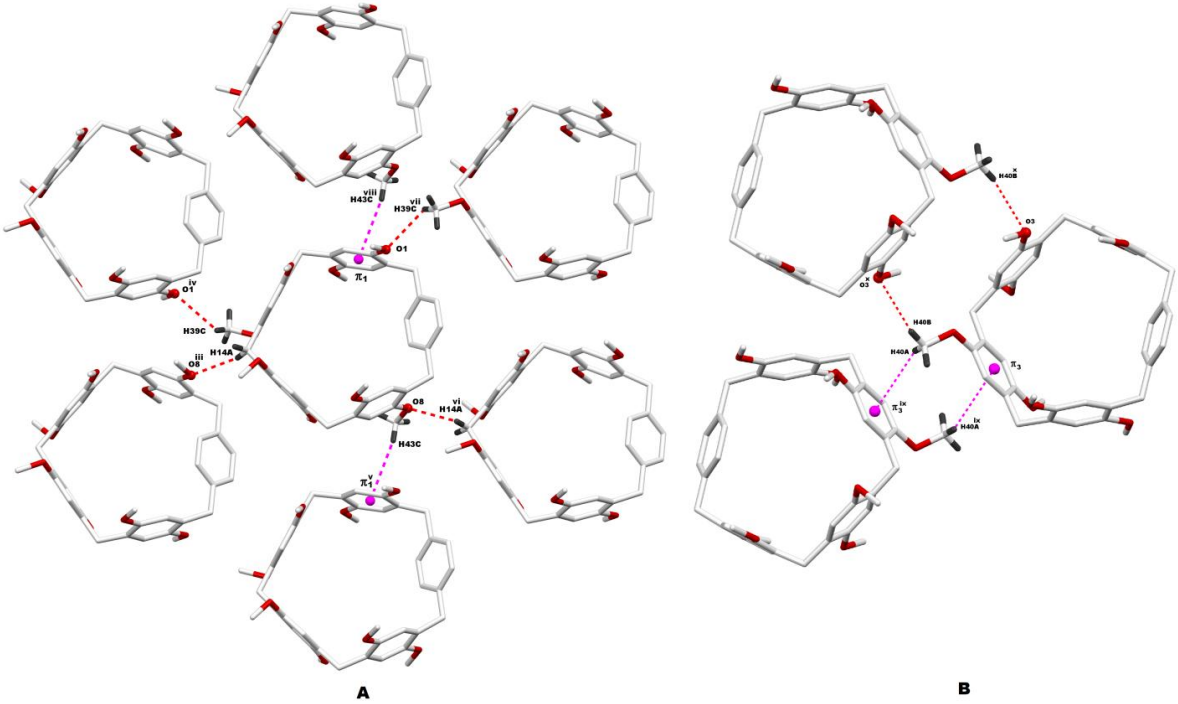


Fig. 4 Intermolecular non-bonding interactions (lateral) observed among a pillar[5]arene molecule with its neighboring symmetry related counterparts in **[1]Ph-ExP5-P** crystals. Symmetry code: [(iii)] 2-x, ½+y, 1.5-z; [(iv)] 1-x, ½+y, 1.5-z; [(v)] 1+x, y, z; [(vi)] 2-x, -½+y, 1.5-z; [(vii)] 1-x, -½+y, 1.5-z; [(viii)] -1+x, y, z; [(ix)] 2-x, 1-y, 1-z; [(x)] 1-x, 1-y, 1-z; π1 & π3 are the centroids of the phenyl rings C1-C6, & C15-C20 respectively.

Table 1: Quantitative details of intermolecular non-bonding interactions observed in **[1]Ph-ExP5-D** crystals (Å, º).

A-B...C	A-B	B...C	A....C	A-B...C
C27-H27···π5^{i}	0.93	3.423	4.341	169.72
C37-H37B···π4^{i}	0.96	2.805	3.703	156.12
C39-H39B···O8^{i}	0.96	2.777	3.70(1)	162.3
C43-H43A···π3^{i}	0.96	3.243	4.168	162.40
C43-H43B··· π5^{i}	0.96	3.380	4.193	132.91
C10-H10···O5A^{ii}	0.93	2.718	3.60(9)	158.6
C28-H28B···O1^{iii}	0.97	3.092	3.781(9)	129.3
C41A-H41B···O4^{iv}	0.96	2.736	3.36(1)	122.9

Symmetry code: $^{(i)}$ 1-x, 1-y, 1-z; $^{(ii)}$ -x, 1-y, 2-z; $^{(iii)}$ -x, 1-y, 1-z; $^{(iv)}$ 1-x, 1-y, 2-z; π3, π4 & π5 are the centroids of the phenyl rings C15-C20, C22-C27 & C29-C34 respectively.

Table 2: Quantitative details of intermolecular non-bonding interactions observed in **[1]Ph-ExP5-P** crystals (Å, º).

A-B...C	A-B	B...C	A....C	A-B...C
C28-H28···O4^{i}	0.97	2.651	3.589(3)	162.9
C37-H37B···π5^{ii}	0.96	2.901	3.831	163.43
C40-H40C··· π5^{i}	0.96	3.084	3.663	120.26
C14-H14A···O8^{iii}	0.97	2.574	3.382(3)	140.8
C39-H39C··· O1^{iv}	0.96	2.818	3.374(4)	117.8
C43-H43C··· π1^{v}	0.96	3.276	4.153	152.80
C40-H40A··· π3^{ix}	0.96	3.200	3.788	121.32
C40-H40B···O3^{x}	0.96	2.789	3.581(4)	140.2

Symmetry code: $^{(i)}$ x, 1/2-y, -1/2+z; $^{(ii)}$ x, 1/2-y, 1/2+z; $^{(iii)}$ 2-x, ½+y, 1.5-z; $^{(iv)}$ 1-x, ½+y, 1.5-z; $^{(v)}$ 1+x, y, z; $^{(ix)}$ 2-x, 1-y, 1-z; $^{(x)}$ 1-x, 1-y, 1-z; π1, π3 & π5 are the centroids of the phenyl rings C1-C6, C15-C20 & C29-C34 respectively.

The crystal packing further highlights the distinct supramolecular organisation adopted by the two crystalline forms. In **[1]Ph-ExP5-D**, the macrocycles are organised into discrete dimeric units along the relevant crystallographic direction (**Fig. S13**, Supporting Information). In **[1]Ph-ExP5-P**, the molecules form one-dimensional supramolecular chains extending along the crystallographic c-axis. These chains are arranged in regular rows along the a-direction, while their packing along the b-direction exhibits a slipped ABAB arrangement (**Fig. S14**, Supporting Information).

Overall, the crystallographic analysis of **[1]Ph-ExP5-D** and **[1]Ph-ExP5-P** reveals a correlation between the macrocyclic conformation, intermolecular interaction patterns, and crystal packing. Differences in the inclination of the individual phenyl rings, macrocyclic cavity height, and centroid-to-corner distances reflect variations in the conformational geometry of the extended pillar[5]arene framework. The **[1]Ph-ExP5-D** structure exhibits greater asymmetry in its macrocyclic dimensions, whereas **[1]Ph-ExP5-P** retains a comparatively regular pentagonal arrangement. These structural differences are accompanied by distinct supramolecular packing

motifs, namely, dimeric association in the former and one-dimensional chain formation in the latter, highlighting the sensitivity of the macrocyclic conformation and solid-state organisation to the crystallisation conditions.

Crystal structures of [1]phenyl-extended pillar[5]arene with guest species

In conventional permethylated pillar[5]arenes, all five hydroquinone derived aromatic units bear two methoxy substituents, resulting in a relatively rigid, pillar-shaped architecture in which the aromatic rings are oriented approximately perpendicular (ca. 90°) to the mean plane of the macrocycle. This conformational constraint may limit the accommodation of relatively bulky aromatic guests within the cavity. In contrast, the phenyl-extended pillar[5]arene **[1]Ph-ExP5** exhibits the ability to encapsulate both toluene and DMF molecules, suggesting that the incorporation of an unsubstituted phenyl unit modifies the conformational preferences of the macrocycle and facilitates guest inclusion.

The crystal structures of **[1]Ph-ExP5.Tol1**, **[1]Ph-ExP5.Tol2**, and **[1]Ph-ExP5.DMF**, featuring different guest inclusion patterns, are shown in **Fig. 1**. Structural analysis reveals distinct guest-to-host stoichiometries and cavity-occupancy patterns across these three crystalline systems. In **[1]Ph-ExP5.Tol1**, the crystallographic composition corresponds to $2(C_{43}H_{46}O_8)\cdot 3(C_7H_8)$, indicating an average of 1.5 toluene molecules per macrocycle. Of these, one toluene molecule is located within the macrocyclic cavity, whereas an additional toluene molecule occupies an external site with 50% occupancy. In contrast, **[1]Ph-ExP5.Tol2** has a host–guest composition of $(C_{43}H_{46}O_8)\cdot 2(C_7H_8)$, with two toluene molecules simultaneously accommodated within a single macrocyclic cavity. The **[1]Ph-ExP5.DMF** crystal structure, with the composition $C_{46}H_{53}NO_9$, contains one DMF molecule included within the macrocyclic cavity of each host molecule.

In **[1]Ph-ExP5.Tol1**, the unsubstituted phenyl ring exhibits a pronounced outward rotation relative to the mean macrocyclic plane, with an interplanar angle of approximately 116° (180° − 63.95°; **Fig. 1** and **Fig. S8**, Supporting information). This conformational deviation produces an enlarged opening at the cavity rim, allowing the aromatic portion of the included toluene molecule to approach the macrocyclic entrance, while its methyl substituent is directed towards the interior of the cavity. The absence of methoxy substituents on this phenyl unit reduces local steric congestion and may facilitate conformational accommodation by the adjacent aromatic units. Consistent with this interpretation, one of the dimethoxy-substituted aromatic rings also exhibits a moderate deviation from perpendicularity, adopting an interplanar angle of approximately 102° relative to the mean macrocyclic plane. The remaining aromatic rings retain orientations close to perpendicular to the macrocyclic plane (**Fig. S8**, Supporting Information).

A distinct guest arrangement is observed in **[1]Ph-ExP5.Tol2**, in which two toluene molecules are co-encapsulated within the same macrocyclic cavity. As in **[1]Ph-ExP5.Tol1**, the unsubstituted phenyl ring is rotated outward, exhibiting an interplanar angle of approximately 122° (180° − 58.05°; **Fig. 1** and **Fig. S8**, Supporting Information). One of the encapsulated toluene molecules is positioned close to this widened cavity opening, with its aromatic ring adopting an approximately perpendicular orientation relative to the plane of the unsubstituted phenyl ring. At the opposite side of the cavity, the second toluene molecule adopts a different orientation, with its aromatic plane approximately parallel to that of the corresponding host phenyl ring near the cavity entrance. These contrasting orientations suggest that the two guest molecules adopt complementary spatial arrangements within the confined cavity. The angle between the aromatic planes of the two encapsulated toluene molecules is approximately 79° (**Fig. S10**, Supporting Information). Despite the incorporation of two guest molecules, the remaining dimethoxy-substituted aromatic rings retain orientations close to perpendicular to the mean macrocyclic plane, with no pronounced conformational deviations. This observation further highlights the structural significance of the unsubstituted phenyl unit in accommodating the included guests without requiring substantial distortion of the remaining macrocyclic framework.

The crystallographic analysis of **[1]Ph-ExP5·DMF** revealed positional disorder of the unsubstituted phenyl ring, with the major and minor orientations refined to occupancies of 73.1% and 26.9%, respectively. The major-occupancy component was considered exclusively in the subsequent analysis of intermolecular interactions. In this component, the unsubstituted phenyl ring is oriented nearly perpendicular to the mean macrocyclic plane, with a dihedral angle of 85.85°. In contrast, the minor-occupancy component adopts an outwardly tilted orientation, corresponding to an angle of 128.71° (equivalent to 180° − 51.29°) relative to the mean macrocyclic plane. This alternative conformation results in an expansion of the macrocyclic cavity, accommodating the DMF guest molecule within the widened cavity (**Fig. S11**, Supporting Information). The dimethoxy-substituted phenyl rings are oriented approximately perpendicular to the mean macrocyclic plane in both major and minor components.

The other macrocyclic dimensions, such as cavity height and cavity width, as well as the dihedral angles between the unsubstituted phenyl ring and its two adjacent dimethoxy-substituted phenyl rings in **[1]Ph-ExP5.Tol1**, **[1]Ph-ExP5.Tol2**, and **[1]Ph-ExP5.DMF**, are provided in the Supporting Information (**Table S3**). These parameters are comparable to those of **[1]Ph-ExP5-P**. The structural features of these complexes underscore the role of the unsubstituted phenyl unit in modulating the cavity geometry and guest-accommodation characteristics of **[1]Ph-ExP5**. Its pronounced out-of-plane rotation, combined with the absence of methoxy substituents, appears to

provide a less sterically congested cavity entrance that facilitates the inclusion of aromatic guests. Particularly noteworthy is the simultaneous encapsulation of two toluene molecules within a single pillar[5]arene cavity, in contrast to the reported inability of the conventional permethylated analogue to accommodate even one toluene molecule within its cavity under comparable conditions. Furthermore, the observation of different host–guest stoichiometries and inclusion arrangements for **[1]Ph-ExP5.Tol1** and **[1]Ph-ExP5.Tol2** indicates that the crystallization conditions may influence guest occupancy and the resulting solid-state supramolecular organization. Differences in solvent composition and guest availability are therefore plausible factors contributing to the distinct inclusion patterns observed in these crystalline systems.

Host-guest and intermolecular interactions in [1]Ph-ExP5 having guest molecules

In the **[1]Ph-ExP5.Tol1**, **[1]Ph-ExP5.Tol2**, and **[1]Ph-ExP5.DMF** host–guest systems, the included guest molecules are stabilized within the macrocyclic cavities by multiple C–H···O and C–H···π non-covalent interactions. These interactions are illustrated in **Fig. 5**, and their geometrical parameters are summarized in **Tables 3–5**.

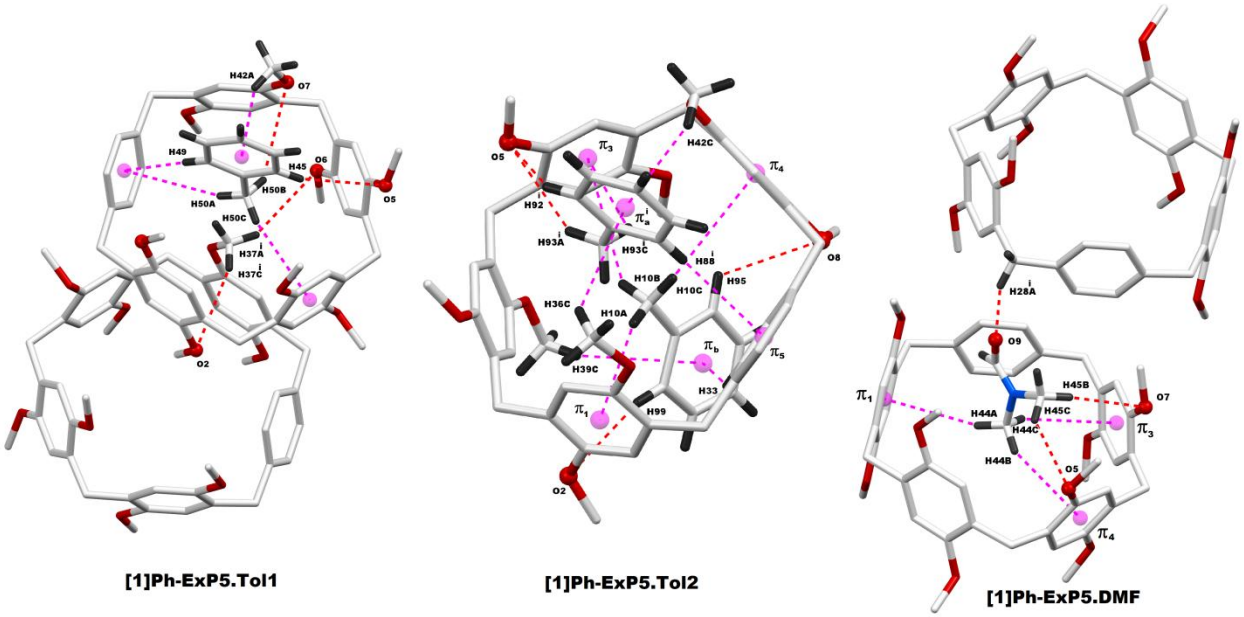


Fig. 5 Demonstration of 1:1 inclusion dimer formed by **[1]Ph-ExP5.Tol1** system by toluene-based and methoxy-based interactions operating within the cavity; Host-guest interactions between two toluene molecules and pillar[5]arene in **[1]Ph-ExP5.Tol2** system and dimeric system formed by **[1]Ph-ExP5.DMF** crystal by DMF-based interactions. Symmetry codes and π-labeling are provided in the corresponding tables.

In the crystal structure of **[1]Ph-ExP5.Tol1**, symmetry expansion reveals a reciprocal methoxy-group inclusion motif between two neighboring pillar[5]arene molecules. Specifically, one

methoxy group from each macrocycle is accommodated within the cavity of the other, resulting in a mutually interlocked 1:1 inclusion dimer, as illustrated in **Fig. 5**. Consequently, each macrocyclic cavity accommodates two distinct types of guest species: a toluene molecule and a methoxy fragment originating from the neighboring pillar[5]arene. This reciprocal inclusion motif contributes to the formation of discrete host–host assemblies within the crystal structure.

The additional toluene molecules occupying external sites in **[1]Ph-ExP5.Tol1** are located near the termini of these inclusion dimers and participate in C–H···π interactions with the surrounding macrocycles (**Fig. 6A**). Their aromatic rings are oriented approximately perpendicular to the mean macrocyclic plane. This arrangement places the external toluene molecules across the cavity openings, suggesting a possible lid-like role in the supramolecular assembly. Furthermore, each external toluene molecule is positioned between two pillar[5]arene molecules belonging to different inclusion dimers, with C–H···π contacts contributing to the association of these neighboring assemblies (**Fig. 6B**). This arrangement is consistent with the crystallographic composition of $2(C_{43}H_{46}O_8)\cdot 3(C_7H_8)$, in which one toluene molecule is included within each macrocyclic cavity, while the additional toluene molecule occupies an external site with half occupancy and is associated with adjacent host molecules. In addition, the methyl group of the external toluene molecule participates in a further C–H···π contact with a third pillar[5]arene, providing an additional interaction within the supramolecular assembly (**Fig. 6B**).

Beyond the reciprocal inclusion interaction with its dimeric counterpart, each pillar[5]arene in **[1]Ph-ExP5.Tol1** exhibits intermolecular non-covalent contacts with five additional neighboring pillar[5]arene molecules in the crystal packing (**Fig. 6C**). The geometrical parameters of these intermolecular contacts are summarized in **Table 3**.

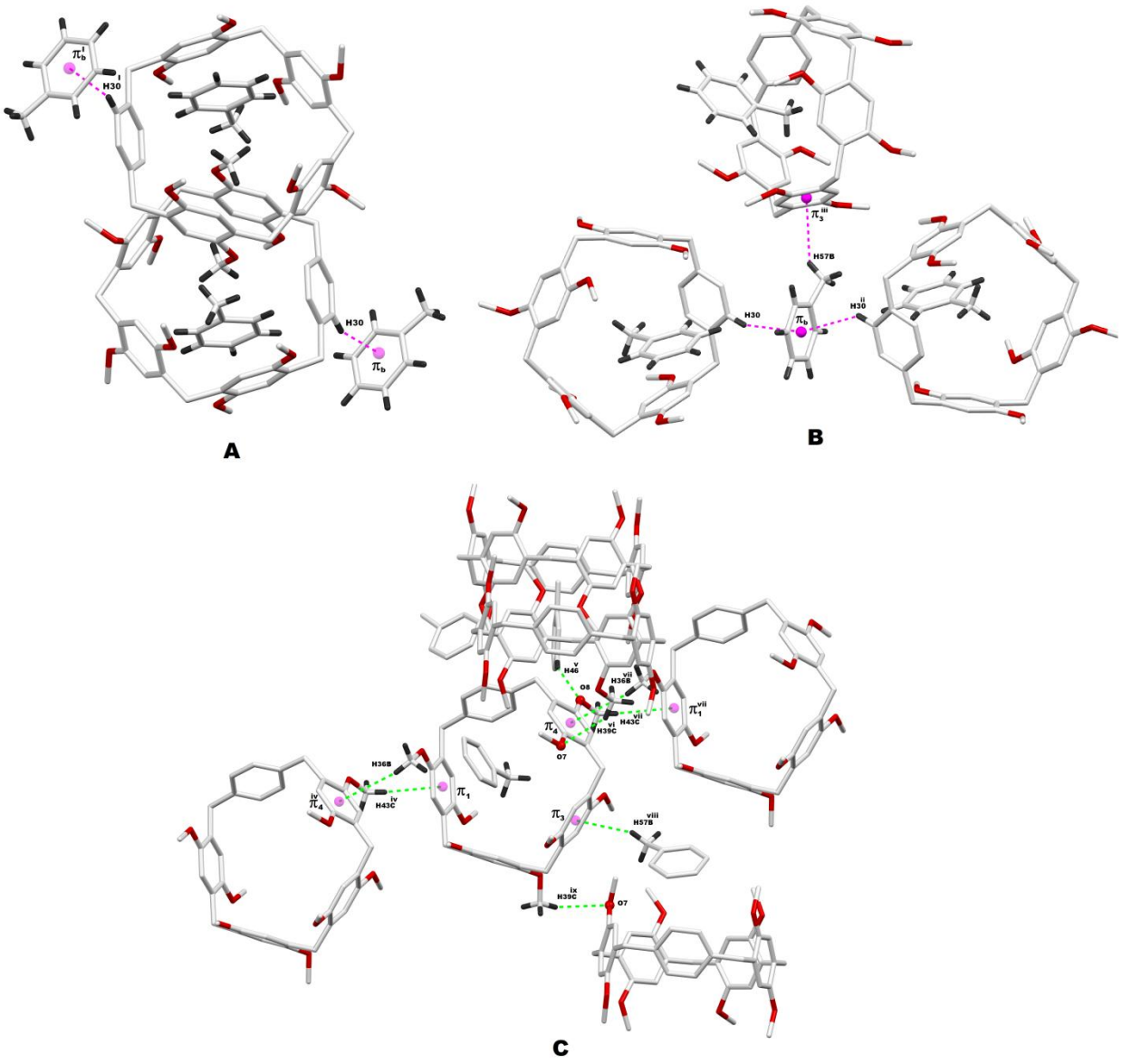


Fig. 6 (A) 1:1 inclusion dimer formed by **[1]Ph-ExP5.Tol 1** system with terminal pyridine molecules; (**B**) A toluene molecule being shared by 3 pillar[5]arene molecules in **[1]Ph-ExP5.Tol1** system; (**C**) intermolecular non-bonding interactions observed between a pillar[5]arene molecule with its neighboring counterparts in **[1]Ph-ExP5.Tol1** crystals. Symmetry code: (i) 1-x, 1-y, 1-z; (ii) 1-x, -y, 1-z; (iii) -1/2+x, ½-y, ½+z; (iv) -1+x, y, z; (v) 1/2+x, ½-y, ½+z; (vi) 1.5-x, -1/2+y, ½-z; (vii) 1+x, y, z; (viii) 1/2+x, ½-y, -½+z;; (ix) 1.5-x, ½+y, ½-z;; π1, π3, π4are the centroids of the phenyl rings C1-C6, C15-C20& C22-C27 and πb is the centroids of the toluene aromatic ring C51-C56 respectively.

Table 3: Quantitative details of host-guest non-bonding interactions and intermolecular non-bonding interactions observed in **[1]Ph-ExP5.Tol1** crystals (Å, °).

A-B...C	A-B	B...C	A....C	A-B...C
C37^{i}-H37A^{i}··· O6	0.96	3.150	4.014(5)	150.3
C37^{i}-H37C^{i}··· O2	0.96	3.341	4.258(5)	160.5
C42-H42A··· πa	0.96	2.689	3.553	150.13
C45-H45··· O5	0.93	3.053	3.959(7)	165.5
C49-H49··· π5	0.93	3.061	3.972	166.79
C50-H50A··· π5	0.96	3.414	4.313	157.01
C50-H50B···O7	0.96	3.445	4.087(7)	126.2
C50-H50C··· π2	0.96	3.252	4.191	165.95
C30-H30··· πb	0.93	2.935	3.817	158.83
C57-H57B··· π3	0.96	2.968	3.756	140.24
C36-H36B··· π4^{iv}	0.96	3.158	4.100	167.22
C39-H39C··· O7^{ix}	0.96	2.690	3.527(4)	145.9
C43-H43C··· π1^{vii}	0.96	2.902	3.836	164.80
C46^{v}-H46^{v}··· O8	0.93	2.685	3.555(8)	156.0
C57-H57B··· π3^{iii}	0.96	2.968	3.756	140.24

Symmetry code: $^{(i)}$ 1-x, 1-y, 1-z; $^{(ii)}$ 1-x, -y, 1-z; $^{(iii)}$ -1/2+x, ½-y, ½+z; $^{(iv)}$ -1+x, y, z; $^{(v)}$ 1/2+x, ½-y, ½+z; $^{(vi)}$ 1.5-x, -1/2+y, ½-z; $^{(vii)}$ 1+x, y, z; $^{(viii)}$ 1/2+x, ½-y, -½+z;; $^{(ix)}$ 1.5-x, ½+y, ½-z;; π1, π2, π3, π4, π5 are the centroids of the phenyl rings C1-C6, C8-C13, C15-C20, C22-C27 & C29-C34 and πa & πb are the centroids of the toluene aromatic rings C44-C49 & C51-C56 respectively.

In contrast, in **[1]Ph-ExP5.Tol2**, the two encapsulated toluene molecules remain confined within the macrocyclic cavity and they do not exhibit identifiable intermolecular contacts with neighbouring pillar[5]arene molecules. Nevertheless, each macrocycle participates in intermolecular non-covalent interactions with four symmetry-related pillar[5]arene molecules in the crystal lattice, as illustrated in **Fig. 7**. The corresponding geometrical parameters are summarized in **Table 4**. Although two crystallographically independent macrocyclic systems are present in the asymmetric unit, only one has been selected as the representative host for illustrating the host–guest interactions and intermolecular contacts discussed herein.

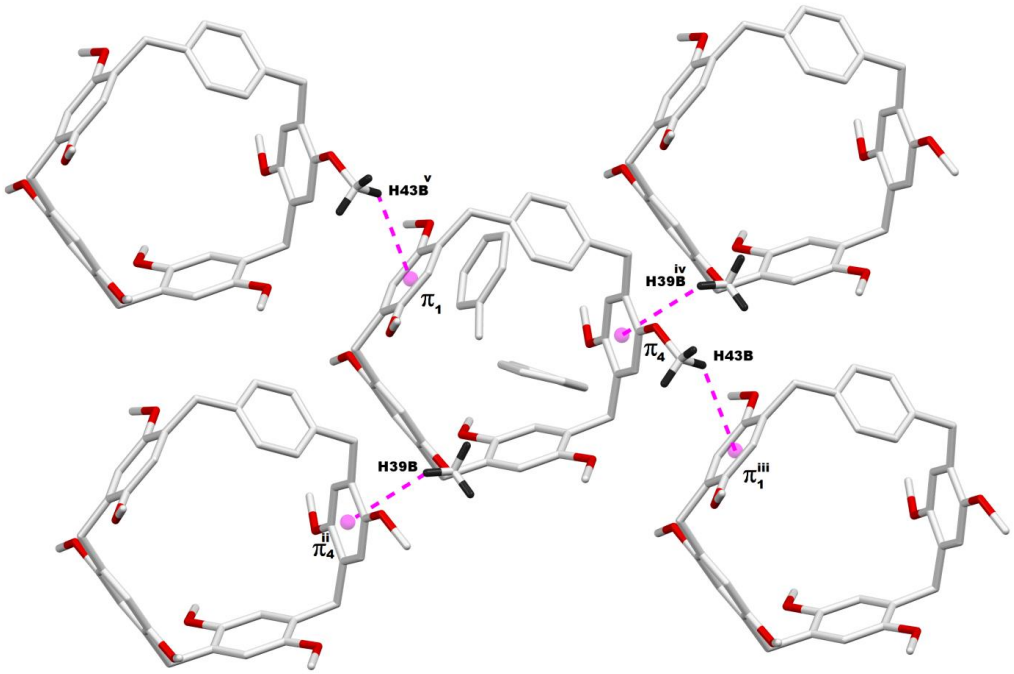


Fig. 7 Intermolecular non-bonding interactions observed between a pillar[5]arene molecule with its neighboring counterparts in **[1]Ph-ExP5.Tol2** crystals. Symmetry code: (ii) 1+x, y, z; (iii) -1+x, -1+y, z;(iv) -1+x, y, z; ;(v) 1+x, 1+y, z; π1& π4 are the centroids of the phenyl rings C1-C6 & C22-C27 respectively.

Table 4: Quantitative details of host-guest non-bonding interactions and intermolecular non-bonding interactions observed in **[1]Ph-ExP5.Tol2** crystals (Å, °).

A-B...C	A-B	B...C	A....C	A-B...C
C88^{i}-H88^{i}··· π5	0.93	2.982	3.875	161.58
C92^{i}-H92^{i}··· O5	0.93	3.436	4.15(1)	135.1
C93^{i}-H93A^{i}···O5	0.96	3.076	3.90(1)	114.5
C93^{i}-H93C^{i}··· π3	0.96	3.390	3.944	118.89
C36-H36C··· πa^{i}	0.96	2.984	3.637	126.49
C42-H42C··· πa^{i}	0.96	2.854	3.744	154.47
C95-H95···O8	0.93	3.138	3.65(1)	116.4
C99-H99···O2	0.93	2.874	3.778(7)	164.3
C100-H10A··· π1	0.96	3.438	3.447(3)	165.74
C100-H100B··· π3	0.96	3.445	4.193	136.58
C100-H100C··· π4	0.96	3.455	4.471	162.60
C33-H33··· πb	0.93	3.448	4.136	132.69
C39-H39C··· πb	0.96	3.411	4.325	159.60
C39-H39B··· π4^{ii}	0.96	3.068	3.929	150.07
C43-H43B··· π1^{iii}	0.96	3.171	3.875	131.59

Symmetry code: (i) 1-x, 1-y, 1-z; (ii) 1+x, y, z; (iii) -1+x, -1+y, z; π1, π3 π4 & π5 are the centroids of the phenyl rings C1-C6, C15-C20, C22-C27 & C29-C34 and πa & πb are the centroids of the toluene aromatic rings C87-C92 & C94-C99 respectively.

The **[1]Ph-ExP5.DMF** crystal structure exhibits a distinct supramolecular assembly in which the DMF molecules participate in interactions involving two symmetry-related pillar[5]arene hosts. Within the primary host cavity, the methyl groups of the encapsulated DMF molecule participate in C–H···O and C–H···π contacts with the surrounding macrocyclic framework, thereby contributing to guest stabilization. In addition, the carbonyl oxygen atom of this DMF molecule participates in an intermolecular O···H–C contact with a neighboring symmetry related pillar[5]arene positioned above the primary host (**Fig. 5**). A reciprocal arrangement is observed for the DMF molecule associated with the second host: its carbonyl oxygen atom participates in an O···H–C contact with the first pillar[5]arene (**Fig. 8A**). Thus, the DMF molecules act as intermolecular connecting species between adjacent macrocycles, giving rise to dimeric supramolecular units.

These dimeric units are further connected to neighboring dimers at both ends through complementary C–H···O contacts, generating one-dimensional supramolecular chains composed of pillar[5]arene–DMF assemblies (**Fig. 8A**). In addition to these chain-forming interactions, each pillar[5]arene participates in lateral contacts with three distinct symmetry-related macrocycles through C–H···O and C–H···π interactions (**Fig. 8B**). The geometrical parameters of the host–guest and intermolecular non-covalent contacts identified in **[1]Ph-ExP5.DMF** are summarized in **Table 5**.

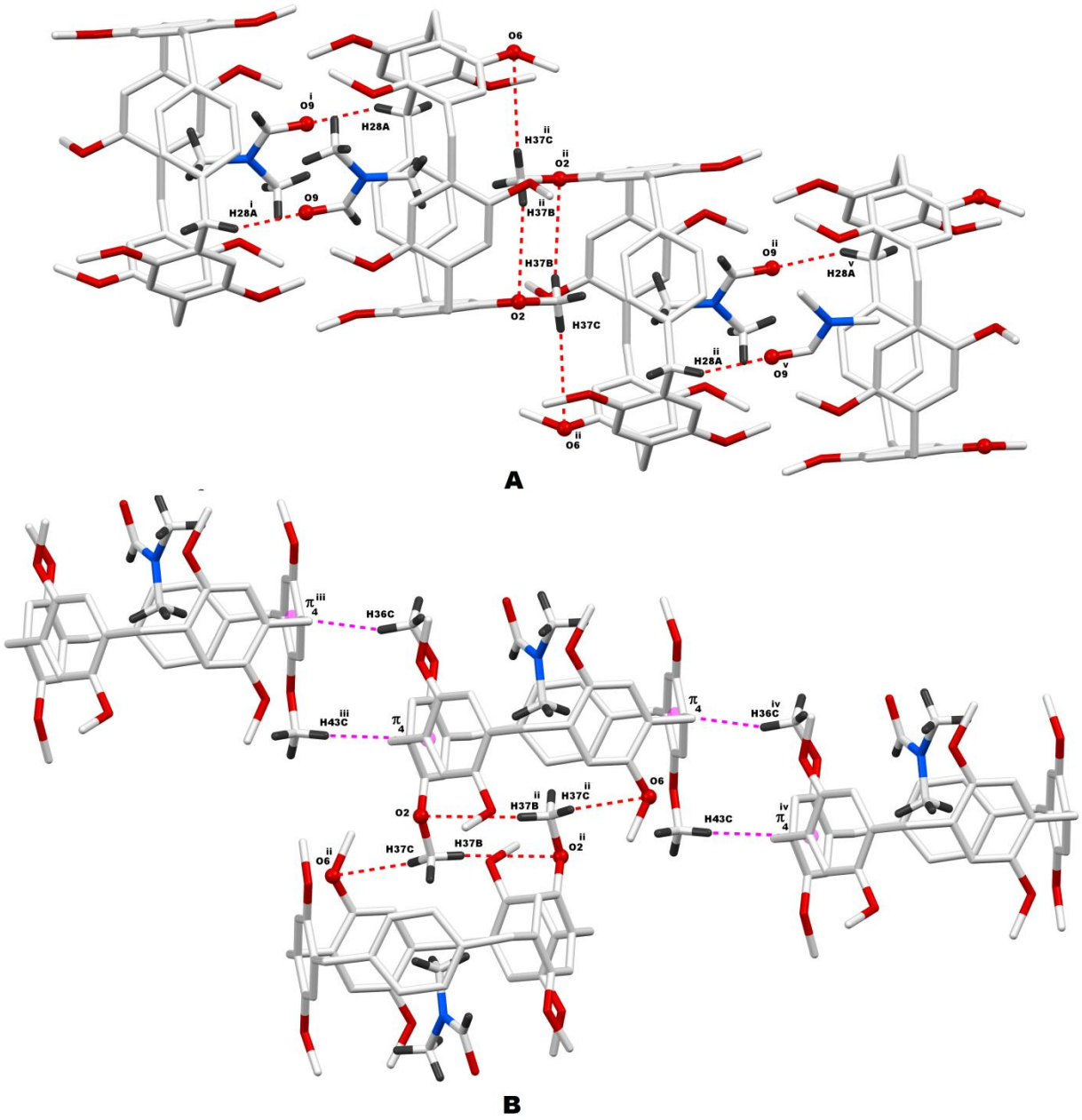


Fig. 8 (**A**) Dimeric system formed by **[1]Ph-ExP5.DMF** crystal by DMF-based and interactions and the consequent linear polymer formation through pillar[5]arene-pillar[5]arene interactions; (**B**) Intermolecular non-bonding interactions (lateral) observed between a pillar[5]arene molecule with its neighboring counterparts in **[1]Ph-ExP5.DMF**. Symmetry code: [(i)] 1-x, 1-y, 2-z; [(ii)] 1-x, 1-y, 1-z; [(iii)] -1+x, y, z; [(iv)] 1+x, y, z; ; [(v)] x, y, -1+z; π4 is the centroids of the phenyl ring C22-C27.

Table 5: Quantitative details of host-guest non-bonding interactions and intermolecular non-bonding interactions observed in **[1]Ph-ExP5.DMF** crystals (Å, º).

A-B...C	A-B	B...C	A....C	A-B...C
C28^{i}-H28A^{i}···O9	0.97	2.77	3.66(1)	153.9
C44-H44A···π1	0.96	3.258	4.186	163.04
C44-H44B···π3	0.96	3.229	4.117	154.66
C44-H44C···π4	0.96	3.368	4.169	142.29
C45-H45B···O7	0.96	2.927	3.86(1)	164.5
C45-H45B···O5	0.96	2.762	3.574(9)	142.7
C36-H36C··· π4^{iii}	0.96	3.130	3.960	145.67
C36-H37B···O2^{ii}	0.96	3.114	3.965(8)	148.6
C36-H37B···O6^{ii}	0.96	3.189	4.142(5)	172.3

Symmetry code: $^{(i)}$ 1-x, 1-y, 2-z; $^{(ii)}$ 1-x, 1-y, 1-z; $^{(iii)}$ -1+x, y, z; π1, π3 & π4 are the centroids of the phenyl rings C1-C6, C15-C20 & C22-C27 respectively.

The differences in host–guest interactions and intermolecular association are reflected in the crystal packing of the three systems, as illustrated in **Figs. S15–S17** (Supporting Information). In **[1]Ph-ExP5.Tol2**, the pillar[5]arene molecules exhibit a comparatively regular arrangement along the crystallographic directions. By contrast, the packing in **[1]Ph-ExP5.Tol1** is more complex, consistent with the formation of reciprocal methoxy-inclusion dimers and their subsequent association through external toluene molecules. In **[1]Ph-ExP5.DMF**, the pillar[5]arene–DMF assemblies form one-dimensional supramolecular chains extending along the crystallographic c-axis. These chains are arranged in regular rows along the a- and b-directions, producing an ordered supramolecular packing pattern.

A particularly noteworthy feature of **[1]Ph-ExP5.Tol1** is the location of the partially occupied external toluene sites within void regions defined by the packing of four surrounding pillar[5]arene molecules. These sites indicate that the crystal structure contains intermolecular void space capable of accommodating additional guest species. The observed external toluene occupancy therefore suggests the potential for guest exchange at these sites under suitable conditions, although the feasibility and selectivity of such exchange would require more experimental verification.

Hirshfeld surface analysis structures

The intermolecular interactions in the crystalline forms of **[1]Ph-ExP5** investigated in this study were further characterized using Hirshfeld surface (HS) analysis [23–24]. The three-dimensional Hirshfeld surfaces mapped over the normalized contact distance (d_{norm}) are presented in **Fig. 9**. The surfaces are predominantly blue, indicating that most intermolecular contacts occur at distances greater than the sums of the corresponding van der Waals radii. However, whitish

regions interspersed with localized red spots are observed around the macrocyclic cavities and rim regions, highlighting areas where intermolecular contacts approach or fall below the sums of the relevant *van der* Waals radii. These features are consistent with the presence of various non-covalent contacts, including C–H···π and C–H···O interactions, identified from the crystallographic structures.

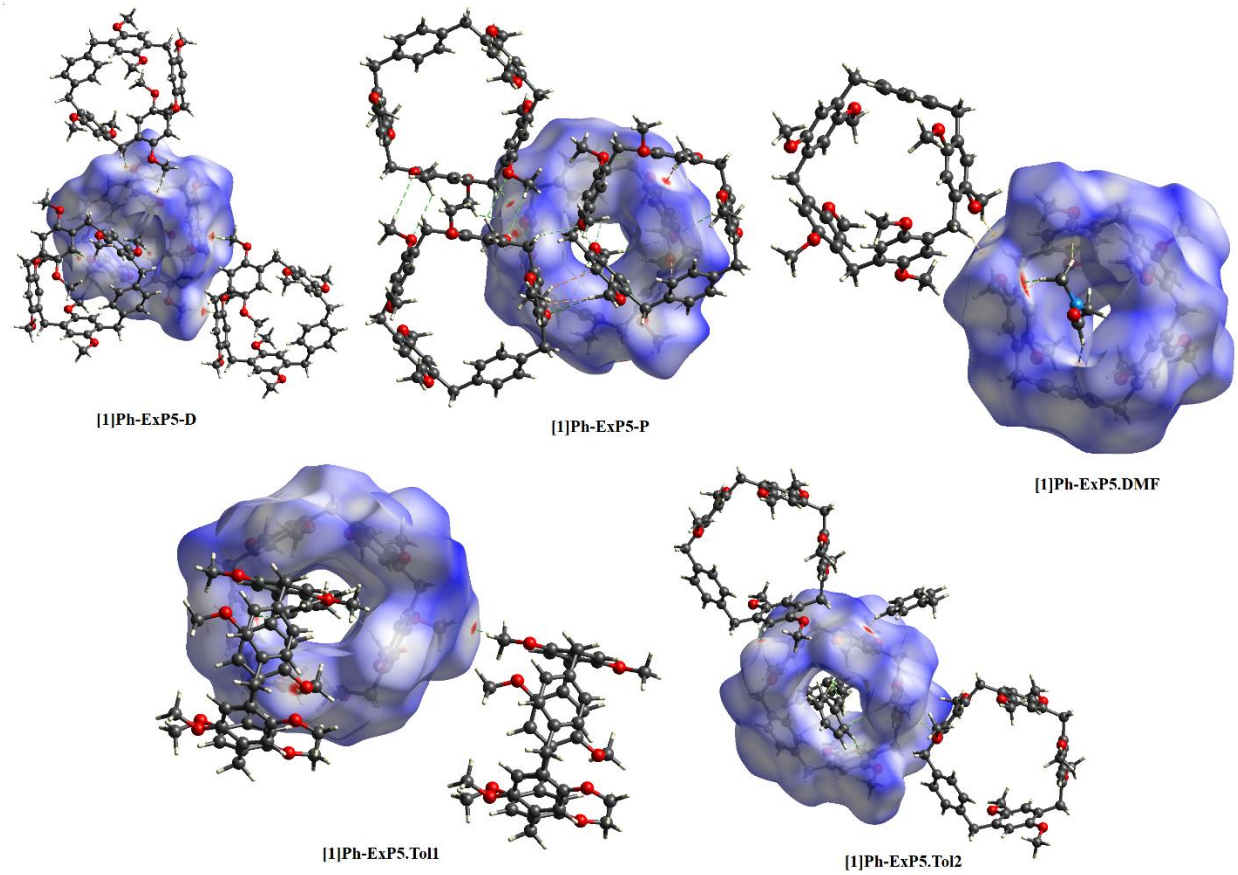


Fig. 9. Hirshfeld surfaces (mapped with dnorm) of the **[1]Ph-ExP5** crystals.

To quantify the relative contributions of different intermolecular contacts, two-dimensional fingerprint plots were generated from the Hirshfeld surface data. The plots reveal that H···H, C···H/H···C, and O···H/H···O contacts constitute the principal contributions to the Hirshfeld surfaces of the investigated **[1]Ph-ExP5** crystals. The relative percentages of these intermolecular contacts, derived from the two-dimensional fingerprint plots, are summarized in **Table 6**. Collectively, Hirshfeld surface analysis enables a quantitative comparison of intermolecular contact distributions across the different crystal structures, complementing the crystallographic analysis of their distinct host–guest and intermolecular non-covalent interactions.

Table 6. Summary of the significant interactions experienced by the **[1]Ph-ExP5** analogues from the 2D fingerprint plots derived from Hirshfeld surface analysis.

Crystal systems	H-H %	C-H %	O-H %
[1]Ph-ExP5_D	64.7	23.2	10.8
[1]Ph-ExP5_P	63.5	25.5	10.9
[1]Ph-ExP5.Tol1	67.9	23.3	8.2
[1]Ph-ExP5.Tol2	67.7	25.8	6.3
[1]Ph-ExP5.DMF	66.1	22.7	10.7

Conclusion

In this study, the structural adaptability and supramolecular assembly of phenyl-extended pillar[5]arene (**[1]Ph-ExP5**) were investigated through single-crystal X-ray diffraction analysis of guest-free and guest-containing crystalline forms obtained under different crystallization conditions. The two guest-free forms exhibit subtle differences in macrocyclic conformation but distinct intermolecular association patterns, resulting in a supramolecular dimer in one form and a one-dimensional supramolecular polymer in the other.

The toluene inclusion complexes demonstrate the ability of **[1]Ph-ExP5** to accommodate either one or two toluene molecules within its cavity, depending on the crystallization conditions. The outward rotation of the unsubstituted phenyl unit appears to facilitate cavity opening and the accommodation of multiple aromatic guests. In contrast, the **[1]Ph-ExP5.DMF** complex forms one-dimensional supramolecular chains composed of dimeric host–guest assemblies, connected through intermolecular C–H···O interactions. Hirshfeld surface analysis further quantifies the intermolecular contact distributions, highlighting the contributions of H···H, C···H/H···C, and O···H/H···O contacts.

Overall, these findings demonstrate that incorporating an unsubstituted phenyl unit into the permethylated pillar[5]arene framework influences its conformational preferences, guest-inclusion behaviour, and intermolecular association. The observed structural diversity highlights the roles of guest identity and crystallization conditions in determining the solid-state organization of phenyl-extended pillar[5]arenes and provides insight into their potential for molecular recognition and guest inclusion.

Funding: This work was supported by Kuwait University Research Administration [Grant No. SC 01/23]. Additional support was provided by the Research Sector Projects Unit (RSPU) at Kuwait University [Grant Nos. GS01/03, and GS03/08].

Author contributions

All authors contributed equally to this work. The manuscript was written through contributions of all authors. All authors have given approval to the final version of the manuscript.

Acknowledgements

The support received from Kuwait University Research Administration and the facilities at the RSPU are gratefully acknowledged.

References

1. Ogoshi T, Yamagishi T-A, Nakamoto Y (2016) Pillar-Shaped Macrocyclic Hosts Pillar[n]arenes: New Key Players for Supramolecular Chemistry. Chem Rev 116:7937–8002.
2. Wang Z-Q, Wang X, Yang Y-W (2024) Pillararene-Based Supramolecular Polymers for Adsorption and Separation. Advanced Materials 36: e2301721.
3. Ohtani S, Kato K, Fa S, Ogoshi T (2022) Host–Guest Chemistry Based on Solid-State Pillar[n]arenes. Coord Chem Rev 462:214503.
4. Li Q, Zhao Y, Huang F (2020) Pillararene-Based Supramolecular Functional Materials. Trends Chem 2:850–864.
5. Strutt NL, Zhang H, Schneebeli ST, Stoddart JF (2014) Functionalizing Pillar[n]arenes. Acc Chem Res 47:2631–2642.
6. Xu X, Jerca V-V, Hoogenboom R (2020) Structural Diversification of Pillar[n]arene Macrocycles. Angew Chem Int Ed 59:6314–6316.
7. Bleus S, Dehaen W (2024) Pillararene-Inspired Arenes: Synthesis, Properties and Applications Compared to the Parent Macrocycle. Coord Chem Rev 509:215762.

8. Wu JR, Wu G, Yang YW (2022) Pillararene-Inspired Macrocycles: From Extended Pillar[n]arenes to Geminiarenes. Acc Chem Res 55:3191–3204.
9. Zhu JY, Gao Y, Rebek J Jr, Yu Y (2025) Recent Applications of Pillararene-Inspired Water-Soluble Hosts. Chem Eur J 31:e202404424.
10. Almoaeen RA, Vinodh M, Alipour FH, Al-Azemi TF (2026) Influence of Crystallization Solvents on the Crystal Structures and Supramolecular Assemblies of a [2]Naphthyl-Extended Pillar[6]arene. CrystEngComm 28:1331–1338.
11. Vinodh M, Almoaeen RA, Alipour FH, Al-Azemi TF (2026) Single-Crystal X-ray Diffraction Study of 1:2 Inclusion Complexes of [2]Biphenyl-Extended Pillar[6]arene with Dichloromethane, 3,5-Lutidine and Ethyl Acetate. Journal of Chemical Crystallography 56:47.
12. Wu JR, Wu G, Zhang L, Li S, Dai D, Yang YW (2022) Guest-Induced Amorphous-to-Crystalline Transformation Enables Sorting of Haloalkane Isomers with Near-Perfect Selectivity. Sci Adv 8:eabo2255.
13. Zeng H, Liu P, Xing H, Huang F (2022) Symmetrically Tetra-Functionalized Pillar[6]arenes Prepared by Fragment Coupling. Angew Chem Int Ed 61:e202115823.
14. Li W, Qin P, Zhao XX, Qu WJ, Lin Q, Yao H, Wei TB, Zhang Y, Liu Y, Shi B (2022) Fluorinated Leaning Pillar[6]arene: Synthesis, Structure and Selective Iodide Anion Binding by Anion–π Interactions. Org Biomol Chem 20:9122–9126.
15. Dai D, Yang J, Zou YC, Wu JR, Tan LL, Wang Y, Li B, Lu T, Wang B, Yang YW (2021) Macrocyclic Arenes-Based Conjugated Macrocycle Polymers for Highly Selective CO_2 Capture and Iodine Adsorption. Angew Chem Int Ed 60:8967–8975.
16. Liu YZ, Wang H, Liu PR, Zhu H, Shi B, Hong X, Huang F (2021) Azobenzene-Based Macrocyclic Arenes: Synthesis, Crystal Structures, and Light-Controlled Molecular Encapsulation and Release. Angew Chem Int Ed 60:5766–5770.

17. Zeng F, Cheng L, Ou GC, Tang LL, Ding MH (2022) Pyromellitic Diimide-Extended Pillar[6]arene: Synthesis, Structure, and Its Complexation with Polycyclic Aromatic Hydrocarbons. J Org Chem 87:3863–3867.
18. Gao B, Tan LL, Song N, Li K, Yang YW (2016) A High-Yield Synthesis of [m]Biphenyl-Extended Pillar[n]arenes for an Efficient Selective Inclusion of Toluene and m-Xylene in the Solid State. Chem Commun 52:5804–5807.
19. Wu JR, Wang CY, Tao YC, Wang Y, Li C, Yang YW (2018) A Water-Soluble [2]Biphenyl-Extended Pillar[6]arene. Eur J Org Chem 2018:1321–1325.
20. Wu JR, Cai Z, Wu G, Dai D, Liu YQ, Yang YW (2021) Bottom-Up Solid-State Molecular Assembly via Guest-Induced Intermolecular Interactions. J Am Chem Soc 143:20395–20402.
21. Wu JR, Mu AU, Li B, Wang CY, Fang L, Yang YW (2018) Desymmetrized Leaning Pillar[6]arene. Angew Chem Int Ed 57:9853–9858.
22. Sheldrick GM (2015) Crystal structure refinement with SHELXL Acta Crystallogr Sect C Struct Chem 71:3-8.
23. Spackman PR, Turner MJ, McKinnon JJ, Wolff SK, Grimwood DJ, Jayatilaka D, Spackman MA (2021) CrystalExplorer: A program for Hirshfeld surface analysis, visualization and quantitative analysis of molecular crystals J Appl Crystallogr 54:1006-1011
24. Turner MJ, McKinnon JJ, Wolff SK, Grimwood DJ, Spackman PR, Jayatilaka D, Spackman MA (2021) CrystalExplorer 21.5 University of Western Australia

Supplementary Files

This is a list of supplementary files associated with this preprint. Click to download.

- SupportinginformationJCCAlazemi20264.docx